Oxidative decarboxylation of fatty acids to terminal alkenes by a membrane-bound metalloenzyme, UndB

Tabish Iqbal[1], Subhashini Murugan[1], Kalpana Rajendran[1], Jagpreet Singh Sidhu[1] and Debasis Das[1]*

[1]Department of Inorganic and Physical Chemistry, Indian Institute of Science, Bangalore, Karnataka-560012, India

KEYWORDS: Membrane protein, Metalloenzyme, Fatty acid decarboxylase, 1-Alkene, Biofuel

ABSTRACT: Biosynthetically produced alkenes are high-value molecules that can serve as 'drop-in' replacements for fossil fuels. Alkenes are also heavily used in the polymer, lubricant, and detergent industries. UndB is the only known membrane-bound fatty acid decarboxylase that catalyzes the conversion of fatty acids to terminal alkenes at the highest reported *in vivo* titers. However, the enzyme remains poorly understood and enigmatic. Here, we demonstrate the first-time purification of UndB and establish that it is an oxygen-dependent, non-heme diiron enzyme that engages conserved histidine residues at the active site. We also identify redox partners that support the activity of UndB and determine the enzyme's substrate specificity and kinetic properties. We detect CO_2 as the co-product of the UndB-catalyzed reaction and provide the first evidence in favor of the hydrogen atom transfer (HAT) mechanism of the enzyme. Our findings decipher the biochemistry of an enigmatic metalloenzyme that catalyzes 1-alkene biosynthesis at the membrane interface with the highest known efficiency.

Introduction

The increasing concerns of global warming related to the use of fossil fuels have triggered enormous interest in the development of biofuels, which are renewable and eco-friendly. Since hydrocarbons such as alka(e)nes are the major components of fossil fuels, their biosynthesis in a sustainable fashion has gained tremendous attention in the past few decades.[1-3] Aldehyde decarbonylation and fatty acid decarboxylation are the two major pathways leading to the biosynthesis of alka(e)nes from the fatty acid precursors (Figure S1).[4, 5] The decarbonylation pathway, which is found in plants, insects, and cyanobacteria, involves the conversion of fatty acid-derived aldehydes to alkanes by aldehyde decarbonylase enzymes.[6-8] The decarboxylation pathway, which is found in several bacterial species and green algae, involves the direct decarboxylation of fatty acids to alka(e)nes by fatty acid decarboxylases.[9-12] Recently, the decarboxylase enzymes have received particular attention because of their ability to produce highly-valuable terminal alkenes in a single-step reaction. Apart from the prospective utility as biofuels, terminal alkenes have extensive application in the polymer, lubricant, and detergent industries (Figure 1A).[13-16] So far, a few fatty acid decarboxylases have been discovered, which differ in their structural and biochemical properties. OleT is the first fatty acid decarboxylase discovered in the bacterium *Jeotgalicoccus* sp.[10] OleT belongs to the class of cytochrome P450 enzymes harboring a heme-iron cofactor in the active site.[10] UndA is another fatty acid decarboxylase, a non-heme diiron enzyme found in several *Pseudomonas* species of bacteria.[11] UndA was initially proposed to be a non-heme mono-iron-containing protein; however, recent spectroscopic and computational studies confirmed the presence of a diiron cluster at the active site of UndA.[17, 18] The third decarboxylase in this category is the fatty acid photodecarboxylase (FAP), which carries out the decarboxylation of long-chain fatty acids to alkanes in a light-dependent manner.[9] The soluble natures of OleT, UndA, and FAP have allowed their rapid biochemical characterization. While OleT prefers to convert long-chain (C12-C20) fatty acids to 1-alkenes[10], UndA decarboxylates medium-chain (C10-C14) fatty acids to 1-alkenes.[11] In 2015, Rui and co-workers discovered a novel membrane-bound fatty acid decarboxylase, UndB, in few *Pseudomonas* species.[12] *In vivo* studies demonstrated that UndB catalyzes the conversion of a broad range of fatty acids (C6-C18) to the corresponding 1-alkenes.[12]

Among 1-alkene-producing enzymes, OleT and UndA are soluble proteins, while UndB is found to be an integral membrane enzyme. *In vivo* studies showed that UndB is more efficient than UndA and OleT.[12, 19] The yield of 1-undecene produced by the *E. coli* cells expressing UndB was at least three-fold higher than that of OleT and UndA.[12] The total yield of 1-alkene produced by the yeast cells expressing UndB was five- to six-fold higher than that of OleT and UndA.[19] Further, the genetically engineered *Pseudomonas aeruginosa* with UndB led to the production of the highest titer of 1-alkene (~1.1 g/L) known to date.[20] An *in vivo* study demonstrated that UndB is capable of bis-decarboxylating diacids, a property similar to OleT.[21] Further, the whole cells expressing UndB were combined with a synthetic catalyst to produce cycloalkenes, demonstrating the importance of UndB as a useful biocatalyst.[21]

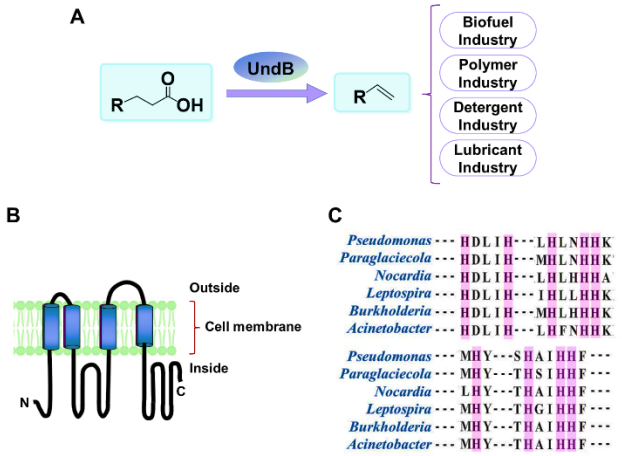

Figure 1. UndB, a membrane-bound fatty acid decarboxylase. (A) Conversion of fatty acids to 1-alkenes by UndB. (B) Predicted transmembrane topology of UndB. (C) Multiple sequence alignment of UndB homologs from different bacterial families. The conserved histidine residues are highlighted in pink boxes. For more details, see Figure S16 and Table S3.

Despite the broader substrate specificity, highest efficiency in the biosynthesis of medium-chain 1-alkenes that can serve as biofuels, and an ability to catalyze the bis-decarboxylation reaction, UndB remains poorly understood. A major challenge in investigating UndB is its membrane-bound nature, which has restricted the successful purification of the enzyme in its active form. Rigorous biochemical characterization and the mechanistic understanding of the enzyme are essential to gain insights into how UndB could be utilized for the large-scale biosynthesis of 1-alkenes from fatty acids that are abundant in nature.[22]

Here, we report the first successful purification of the integral membrane enzyme, UndB, following its heterologous overexpression in *E. coli*. We establish that UndB is an oxygen- and redox-dependent enzyme that converts fatty acids to terminal alkenes and releases CO_2 as the C1-derived co-product. We reconstitute the activity of UndB *in vitro* using biological and chemical redox partners and establish an efficient redox couple for UndB. We also demonstrate, for the first time, that iron is the active metal in UndB. Further, we establish the substrate specificity and kinetic properties of the enzyme and postulate that the UndB-catalyzed reaction proceeds via a hydrogen atom transfer (HAT). Our study provides insight into how UndB catalyzes a chemically challenging conversion of fatty acids to 1-alkenes at the membrane interface and furnishes a platform for the future applications of UndB in biofuel and chemical industries.

Results

UndB is a diiron-containing integral membrane enzyme

We selected UndB from *Pseudomonas mendocina* ymp (*Pmen_4370*) for our investigation as this homolog of UndB (*Pm*-UndB, UniProt ID: A4Y0K1) was reported to be the most efficient in converting lauric acid (LA) to 1-undecene *in vivo*.[12, 19, 20] *Pm*-UndB is a 352-amino acid-containing protein with four predicted transmembrane helices (TMHs) (Figure 1B) present at the residue positions 39-60 (TMH1), 67-85 (TMH2), 185-205 (TMH3), and 228-245 (TMH4). Both the N- and C- terminus of UndB are predicted to be in the cytosol. UndB does not share any sequence similarity with the previously reported fatty acid decarboxylases such as OleT, FAP, or UndA. The primary sequences of UndB and its homologs show conserved histidine-rich motifs that are typically found in the membrane-bound diiron enzymes belonging to the family of fatty acid desaturases/hydroxylases (FADH) (Figure 1C) (Figure S2).[23] Based on this similarity, UndB is suggested to be a membrane-bound diiron-enzyme.[12] Phylogenetic analysis of *Pm*-UndB with other identified members of the FADH family shows that UndB is closely related to a yeast enzyme, delta (7)-sterol 5(6)-desaturase (ERG3, UniProt ID: P32353) (Figure S3). [24] However, ERG3 lacks any biochemical, structural, or mechanistic characterization. The stearoyl acyl CoA desaturase-1 (SCD1) from *Mus musculus* is the only enzyme in the FADH family, which is biochemically and structurally characterized to date.[25, 26] Enzymes of the FADH family carry out a wide variety of C–H activation chemistries[27, 28], with a few examples of C–C bond formation.[29] It is noteworthy that UndB and the poorly characterized plant aldehyde decarbonylase (CER1)[6] are the only enzymes of the FADH family known to catalyze the C–C bond cleavage reactions. However, there are no mechanistic insights of how these enzymes catalyze such challenging reactions. The previously reported studies of UndB were all carried out with the whole cells expressing the enzyme[12, 19-21], and the enzyme, so far, could not be purified to homogeneity. To obtain in-depth knowledge of UndB, isolation and purification of the enzyme are essential, which remain challenging due to the membrane-bound nature of the enzyme.

We overexpressed UndB in *E. coli* with a fusion tag and a His_8 tag (see Supporting Information). We employed the non-ionic detergent lauryl maltose neopentyl glycol (LMNG) to solubilize the protein from the membrane of the cells expressing the protein. Subsequently, the protein was purified using affinity chromatography (see Supporting Information). The purified protein appeared as a single band on SDS-PAGE and eluted mainly as a single peak on the size exclusion chromatography (SEC) column, confirming the purity (>95%), homogeneity, and monomeric state of the protein (Figure 2A-B).

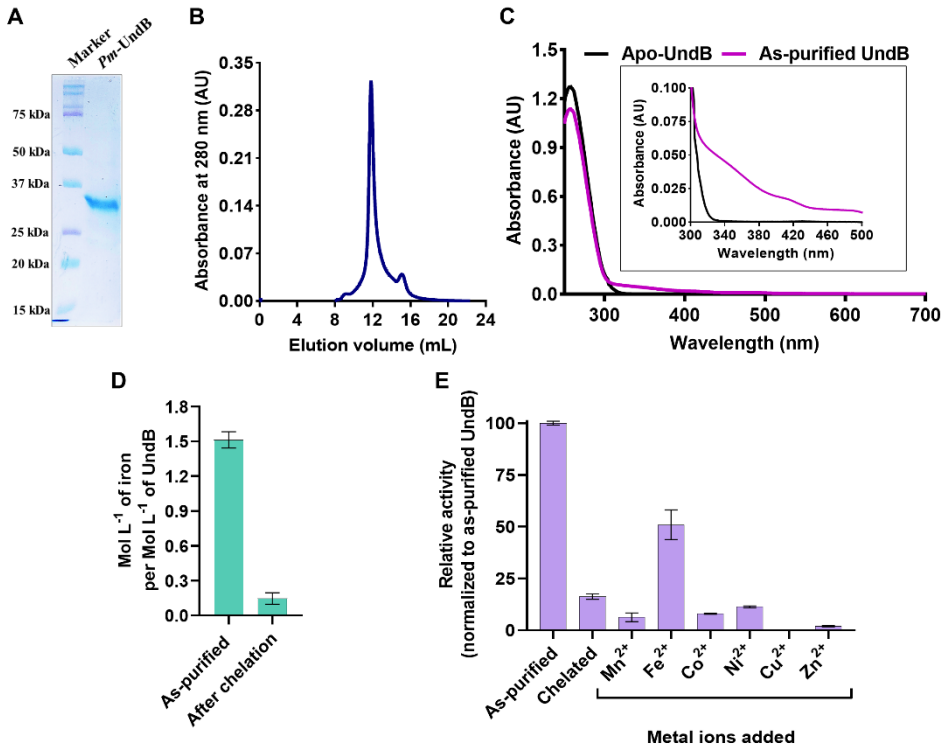

Figure 2. Purification and metal-characterization of UndB. (A) SDS-PAGE analysis of the purified UndB. The uncropped image is available in Figure S25. (B) Size exclusion chromatography (SEC) elution profile of UndB in LMNG. (C) UV-visible spectrum of the as-purified UndB (pink) and apo-*Pm*-UndB (black) (inset: expansion of 300 nm - 500 nm region). (D) ICP-MS analysis of the iron content of as-purified UndB and chelated UndB. (E) Activity analysis of as-purified UndB, chelated UndB, and chelated UndB in the presence of various metal ions. The activity of UndB was measured with lauric acid (LA) as a substrate. For Figure 1D-E, error bars represent the standard deviation (s.d.) of triplicate (n=3) data.

The UV-visible absorption spectrum of the purified protein exhibited a minor yet broad peak at ~340 nm (Figure 2C), which is a signature feature of the diiron proteins, including aldehyde deformylating oxygenases (ADO), SCD1, and UndA.[17,26,30] The extinction coefficient of UndB at 340 nm was found to be 6.8 mM^{-1} cm^{-1}, which is similar to the value reported for SCD1 (6.1 mM^{-1} cm^{-1}).[26] The metal content of the purified protein was measured using inductively coupled plasma mass spectrometry (ICP-MS) and inductively coupled plasma optical emission spectrometry (ICP-OES). Using both methods, we found that each mol/L of the purified UndB contains ~1.5 mol/L of iron, which translates to ~75 % of the protein occupied with iron considering two metal ions present per active site of the protein (Figure 2D) (Table S1). In a complementary experiment, we utilized the ferrozine-based colorimetric assay to quantify iron content in the purified UndB. Ferrozine binds to Fe^{2+} to generate a chelate complex that exhibits an absorbance at 562 nm.[31] Iron quantification from the ferrozine assay was also in accordance with the ICP-based measurements (Table S1), establishing the presence of a diiron center in the enzyme. To explore the role of iron in the activity of UndB, we chelated the iron content of the enzyme with various chelating agents such as ferrozine, ascorbate, EDTA, TPEN, and dipicolinic acid. UV-visible spectroscopic analysis of the resulting apoenzyme exhibited a loss of the peak at 340 nm. (Figure 2C). Further, we found that the chelated UndB lost the majority of its iron content and activity. The chelated UndB was found to contain only ~0.15 mol/L of iron per mol/L of the enzyme, which led to a ~83 % loss in activity (Figure 2D-E). We further supplemented the chelated UndB with various divalent metal ions. We found that only with the addition of iron UndB regained its activity, whereas all other metal ions failed to support the activity of the enzyme (Figure 2E). These results provide the first experimental evidence that UndB is a non-heme diiron enzyme.

Conserved histidine residues are essential for iron binding at the active site of UndB

UndB harbors histidine-rich motifs comprised of nine histidine residues that could serve as ligands for the diiron center of the enzyme. These conserved histidine residues are characteristic features of the members of the FADH family, such as SCD1.[23] Based on the multiple sequence alignments of UndB with its homologs from different organisms (Figure 1C) and with SCD1 and FAH (Figure S2), we identified the conserved histidine residues of UndB. To probe whether these histidine residues are essential for the activity of UndB by coordinating the diiron center of the enzyme, we generated alanine mutants of six conserved histidine residues, namely H86A, H90A, H125A, H128A H294A, and H297A. We found that none of the mutants exhibit detectable activity (Figure 3A), suggesting that UndB engages conserved histidine residues at the active site as ligands for the diiron center of the enzyme.

Recently, the crystal structure of mouse SCD1 (PDB ID: 6WF2) displayed nine histidine residues forming the coordination spheres of the diiron center.[26] To probe whether the histidine residues of the histidine-rich motifs of UndB are present in the enzyme's active site, we modeled the structure of *Pm*-UndB by AlphaFold2 using the ColabFold server (Figure 3B).[32, 33]

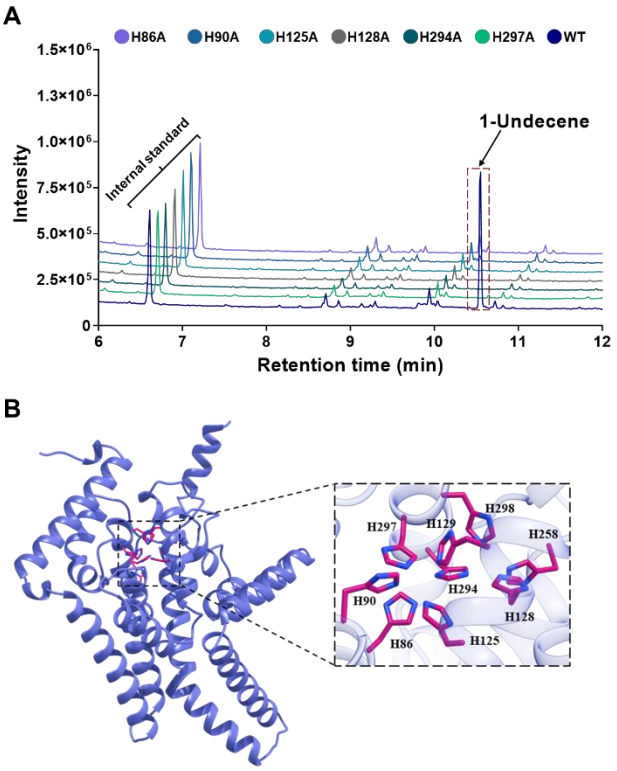

Figure 3. Modeled structure and mutational analysis of UndB. (A) Stacked GC-MS chromatographs of activity analysis of the wild-type (WT) UndB and the alanine mutants of UndB with lauric acid. The product, 1-undecene, elutes at 10.6 min. 1-Nonene was used as an internal standard, which elutes at 6.6 min. (B) 3D-structure of UndB modeled with AlphaFold2 using the ColabFold server at the default settings. The conserved histidine residues proposed for binding the diiron center of *Pm*-UndB are shown in the zoomed-in image.

Further, the transmembrane regions of the enzyme were assessed using the PPM 2.0 web server.[34] The modeled structure of the *Pm*-UndB exhibits four transmembrane helices (TMH1-TMH4) (Figure S5). The global fold of the modeled structure of UndB was also compared to that observed in SCD1 (PDB ID: 6WF2, 4YMK)[25, 26] and yeast fatty acid hydroxylase (PDB ID: 4ZR1)[35], the only two structurally resolved members of the FADH family (Figure S5). All three proteins adopt a mushroom-like fold, where transmembrane helices constitute the stem, and the cytosolic domain forms the mushroom crown. Interestingly, we found that the nine histidine residues of UndB in the modeled structure are clustered at the cytosolic domain, possibly forming the binding site of the diiron center (Figure 3B). Our findings are corroborated by the site-directed mutagenesis experiments that we conducted, which confirmed the presence of these histidine residues at the active site of UndB. Importantly, our study also validates the accuracy of our predicted model, as evidenced by the success of our site-directed mutagenesis studies.

Screening and identification of optimal redox partners for UndB

Diiron enzymes depend on redox partners and external sources of electrons for multiple turnovers. For example, the *in vitro* activity of SCD1 is supported by the cytochrome b5 (Cb5)/cytochrome b5 reductase (Cb5R)/NADH system.[26] While the *in vivo* activity of UndB has been previously studied, it is important to note that the activity was measured in the context of whole cells expressing the enzyme, where intracellular electron sources and electron transfer proteins may have provided support for the enzyme's function.[12, 19-21] A study performed in yeast showed that co-expression of various electron transfer proteins led to a ~40-100 % increase in the *in vivo* activity of UndB.[19] Thus, the availability of efficient redox partners is essential for the optimal activity of redox-dependent enzymes.

To obtain the *in vitro* activity with the purified UndB, we employed Fdx (Fdx) coupled with FNR (FNR) (see Supporting Information). FNR is a FAD-containing protein that oxidizes NADPH, the physiological electron donor, and reduces the [Fe-S] cluster containing Fdx (for more details on Fdx and FNR used in this study, see Supporting Information Figure S6-S7, Table S2). Our activity analysis of UndB in the presence of redox partners Fdx/FNR/NADPH showed that this system efficiently supports the *in vitro* activity of UndB (Figure 4A).

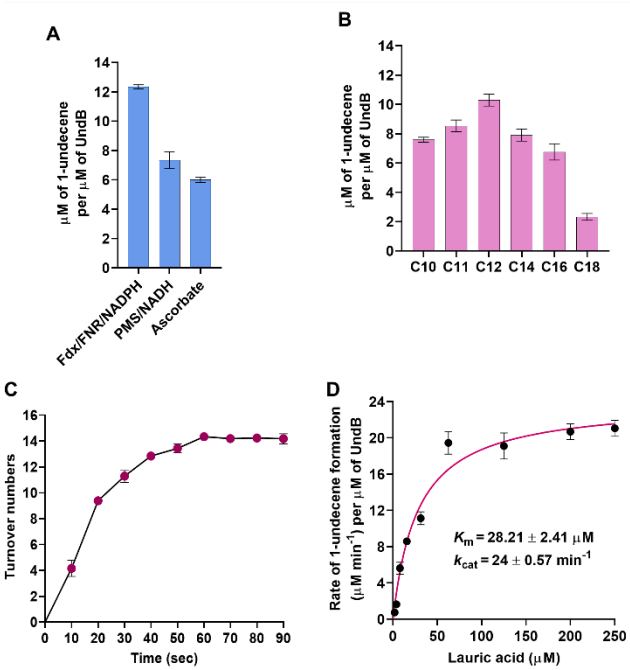

Figure 4. Activity analysis of UndB. (A) Activity of UndB in the presence of Fdx/FNR/NADPH, PMS/NADH, and ascorbate. Other tested chemicals were unable to support the activity of the enzyme. (B) The substrate specificity of UndB with fatty acids of various chain lengths (C10-C18). Error bars in (Figure 4 A-B) represent the standard deviation (s.d.) of quartet (n=4) data. (C) Time-course of 1-undecene formation from lauric acid (LA) by *Pm*-UndB. (D) Michaels-Menten kinetics of UndB with varying concentrations of LA. Error

bars in (Figure 4 C-D) represent the standard deviation (s.d.) of two experiments performed in triplicates (n=6).

Apart from the biological redox partners, we also tested the efficacy of several chemical redox partners such as phenazine-methosulphate (PMS)/NADH, methyl-viologen/dithionite, ascorbate, dithiothreitol (DTT), flavin adenine dinucleotide (FAD)/NADPH and riboflavin/NADPH and dithionite, in supporting the activity of UndB; as some of these chemical redox partners have been shown to support the activities of various diiron enzymes including UndA and ADO.[11, 30] In our screening, we found that PMS/NADH and ascorbate were the only tested chemicals that supported the activity of UndB (Figure 4A); albeit to a lesser extent compared to the Fdx/FNR/NADPH system. Therefore, we employed Fdx/FNR/NADPH system in all subsequent experiments with UndB.

Substrate specificity and kinetics properties of purified UndB

Due to the challenges associated with the purification of the membrane-bound UndB, there is scant knowledge about the kinetic properties and substrate specificity of UndB. Our strategy of purifying UndB to homogeneity and finding a suitable redox system (Fdx/FNR/NADPH) that supports *in vitro* activity and multiple turnovers of the enzyme led us to perform a detailed activity analysis of the enzyme. Our initial enzyme activity optimization studies showed that UndB has the optimal activity at pH 8.0 and the temperature 25 °C (Figure S8). Under these conditions, UndB activity was assessed with a wide range of fatty acid substrates (chain length C10-C18). The enzyme displayed a preference for lauric acid (C12 fatty acid) compared to either the longer- or shorter-chain fatty acids (Figure 4B). With stearic acid (C18 fatty acid), UndB showed substantially poor activity compared to the other fatty acids tested. These results demonstrate that UndB prefers the medium-chains over the long-chain fatty acids, which is in accordance with the previously reported *in vivo* activity of UndB.[12]

Next, we sought to establish the kinetic properties of UndB as there is no kinetic information on the enzyme to date. In the presence of lauric acid as the substrate and optimal redox system, we found that UndB achieves a maximum turnover of ~14 in ~1 min (Figure 4C), after which the reaction stalled, suggesting the possibility of inactivation of UndB. Recently, similar observations were also reported with the membrane-bound SCD1.[26] However, in this case, the reaction stalled after ~10 min, but the total turnover numbers (TTN) remained ≤8. We performed the Michaelis–Menten kinetic measurements of UndB using the initial rates derived from the first 30 s of the reaction. We found that the K_m of the enzyme for LA is 28.20 ± 2.41 μM, and the k_{cat} is 24 ± 0.57 min^{-1} (Figure 4D). The TTN (≥14) and turnover frequency (TOF, ≥24 min^{-1}) achieved by UndB are comparatively higher than the other known non-heme diiron fatty acid decarboxylase, UndA, with LA (TTN ≤6.5 and TOF ≤3.6 min^{-1}).[11] These observations confirm that UndB has higher efficiency of 1-undecene production from LA than UndA. Further, our results demonstrate that UndB is a relatively fast-acting enzyme compared to UndA, OleT, and ADO for producing medium-chain hydrocarbons.[11, 36, 37] This is the first report of the kinetics studies of UndB, and our findings can further guide engineering and optimizing the reaction system for more efficient production of 1-alkenes.

UndB is an oxygen-dependent enzyme that releases CO_2 as the co-product

UndA, the only other known diiron-containing fatty acid decarboxylase, is an oxygen-dependent enzyme.[11, 17, 38] It has been established that UndA is inactive in the absence of oxygen; however, no information is available on the oxygen dependency of UndB. Given that other diiron enzymes, such as SCD1, UndA, and ADO, are known to be O_2-dependent, and the oxygen activation at the substrate-bound diiron center is the first step of the catalysis of these enzymes[11, 38, 39], we hypothesize that it would be unlikely for UndB to catalyze the fatty acid decarboxylation reaction without O_2. Therefore, to explore the dependency of UndB on O_2, we performed activity assays of the enzyme under anaerobic conditions using a Schlenk line and repeated cycles of vacuum and nitrogen. The reactions were carried out either in the absence of oxygen ($-O_2$) or after starting the reaction under anaerobic conditions; the reaction mixture was brought under the atmospheric oxygen ($-O_2$, then $+O_2$). As a positive control, a reaction was started and carried out under atmospheric oxygen ($+O_2$). We found that the activity of UndB was substantially decreased (~84 %) in the absence of O_2 ($-O_2$) compared to the activity of the enzyme under atmospheric oxygen ($+O_2$) (Figure 5A). The residual activity of the enzyme could be attributed to the residual oxygen in the reaction, which could not be removed under the experimental conditions. When the enzyme assay was initiated under anaerobic conditions and brought under the atmospheric oxygen ($-O_2$, then $+O_2$), ~70 % of enzyme activity was regained compared to the positive control (Figure 5A). These results establish that the activity of UndB is dependent on O_2.

We also investigated whether UndB could utilize peroxides as alternatives to O_2 and electrons to perform catalysis. We observed that peroxides such as H_2O_2 and di-tert-butyl peroxide (DTBP) did not support the enzyme's activity, suggesting that UndB does not undergo the peroxide shunt pathway (Figure 5A).

To further elucidate the mechanism of UndB-catalyzed reaction, we investigated the fate of the C1 carbon upon cleavage of the C1−C2 bond of the fatty acid by UndB. The nature of the C1-derived co-product can shed light on the mechanism of the enzyme. In analogy to other soluble diiron enzymes such as UndA or ADO that perform C−C bond scission, we anticipated that the co-product of UndB-catalyzed reaction could be either CO_2 or formate[11, 40]. If the co-product is CO_2, UndB might follow a mechanism similar to UndA or OleT, and the reaction may involve a HAT from the C-β position or a proton-coupled electron transfer (PCET) from the carboxyl group (Kolbe's-like decarboxylation) of the substrate.[38, 41-44] If the co-product is formate, UndB might follow a mechanistic plot similar to ADO mechanism.[39, 45, 46]

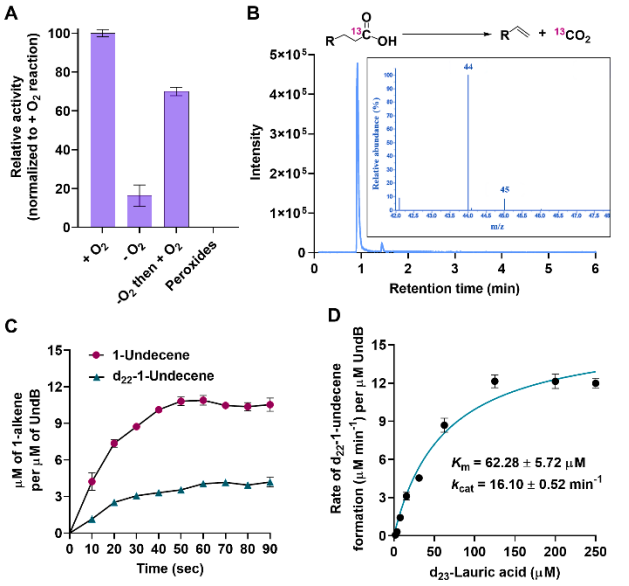

Figure 5. Mechanistic investigation of UndB. (A) Oxygen and peroxide dependency of UndB. Activity assays of UndB were started and carried out under atmospheric oxygen ($+O_2$); started and carried out under anaerobic condition ($-O_2$); started under anaerobic condition, and brought under the atmospheric oxygen ($-O_2$ then $+O_2$); or performed in the presence of peroxides (H_2O_2 or DTBP). Error bars in (Figure 5A) represent the standard deviation (s.d.) of triplicate (n=3) data. (B) Detection of CO_2 as the C-1 derived co-product of UndB-catalyzed reaction. GC chromatogram of the reaction headspace of the UndB reaction carried out with 1-^{13}C-LA as substrate. Inset shows the mass spectrum of the peak at 0.95 min, corresponding to $^{13}CO_2$ (m/z= 45) and CO_2 (m/z= 44). (C) Time-dependent formation of 1-undecene and d_{22}-1-undecene in the UndB reaction containing 500 μM of each LA and d_{23}-LA. (D) Michaels-Menten kinetics of UndB with d_{23}-LA. Error bars in (Figure 5 C-D) represent the standard deviation (s.d.) of two experiments performed in triplicates (n=6).

Therefore, we first investigated the possibility of forming formate as the C1-derived co-product of UndB reaction. We employed 2-nitrophenylhydrazine (2-NPH) to derivatize formate, which can be analyzed by HPLC (Supporting Information).[47] In our experiments, a small amount of formate (~35 μM) was detected in the enzyme assay, however, a similar amount of formate was also detected in the control assays that lacked the enzyme or NADPH (Figure S9). Further, the amount of formate detected in the enzyme assays did not correspond to the amount of 1-undecene produced (217 μM) in the same reaction. These observations suggest that the detected formate was not produced in the enzyme reaction but was present in all the samples as an environmental contaminant. Subsequently, we investigated the possibility of the formation of CO_2 as the co-product of the UndB-catalyzed reaction. For this, we performed the UndB reactions with 1-^{13}C-labeled lauric acid (1-^{13}C-LA) as a substrate. GC-MS analysis of the headspace of this reaction showed a new signal corresponding to $^{13}CO_2$ at m/z = 45 in addition to the signal at m/z = 44 originating from the environmental CO_2 (Figure 5B). The GC-MS signal corresponding to $^{13}CO_2$ was not present in the control experiments lacking UndB or NADPH, confirming that CO_2 is the C-1-derived co-product of the UndB-catalyzed reaction (Figure S10).

Proposed hydrogen atom transfer-mediated initiation of UndB catalysis

Fatty acid decarboxylases may use distinct decarboxylation mechanisms to produce terminal alkenes and CO_2. Heme containing OleT, the most studied fatty acid decarboxylase to date, is proposed to initiate the reaction via a HAT from the C-β of the substrate to generate a substrate radical.[41] The mechanism of OleT differs from the other well-known CYP450s because OleT does not follow the oxygen rebound mechanism following HAT.[44] Various computational and experimental studies have suggested that the active site residues of OleT are fine-tuned to allow the enzyme to elude the oxygen rebound mechanism.[44, 48] The HAT step is proposed to be followed by an electron transfer to compound II, leading to the C–C bond scission with the concomitant release of CO_2 and terminal alkene (Figure S11).[41-44] In a recent study with the diiron-containing soluble fatty acid decarboxylase UndA, two reactive intermediate species have been identified and characterized using the stopped-flow and freeze-quenched spectroscopic techniques.[38] Based on these observations and the analogy with the other soluble diiron enzymes, a mechanism was proposed for UndA. The mechanism starts with the binding and activation of the molecular oxygen at the diiron center of the enzyme to generate a μ-peroxo-Fe_2(III/III) species, which would initiate the reaction via a HAT from the C-β of the fatty acid leading to the formation of 1-alkene and CO_2 (Figure S12). Alternatively, a Kolbe's-like decarboxylation was also proposed, which would initiate with a proton-coupled electron transfer (PCET) from carboxyl group of the fatty acid. However, there is currently no direct evidence of whether the HAT or the Kolbe's-like decarboxylation mechanism is operant by UndA to date.[17, 38]

Based on these analogies and the similarity of UndB with the fatty acid desaturases, a mechanism of UndB can be proposed. In this mechanism, the diiron (III) core of the resting enzyme would bind to the fatty acid substrate followed by the activation of molecular oxygen in the presence of external electrons, possibly via Fdx or an unidentified partner protein, to yield the oxo-diiron (IV) species. This species could initiate the reaction by HAT from the C-β of the fatty acid to generate a substrate radical and an oxo-diiron (III/IV) species (Figure S13). Alternatively, a Kolbe's-like decarboxylation mechanism could also be operant, which would proceed through proton-coupled one-electron oxidation of the carboxyl group of fatty acid, leading to the formation of a carboxyl radical. This substrate-based carboxyl radical could release CO_2 and 1-alkene from the active site (Figure S14).

To explore the mechanistic plot of UndB catalysis, we performed kinetic isotope effect studies of the enzyme with the deuterium-labeled substrate. We performed the reaction of UndB with the fully deuterated lauric acid (d_{23}-LA), which yielded the fully deuterated 1-undecene (d_{22}-undecene) with the loss of one deuterium from the substrate (Figure S15A-D). Interestingly, the yield of the deuterated product was ~17 % less compared to the 1-undecene produced from the unlabeled lauric acid (Figure

S15E). We subsequently performed a competition assay by incubating UndB with both the unlabeled LA and d_{23}-LA (500 μM each) in a single reaction and measured the product formation over 90 sec. If the HAT mechanism is operant, it should exhibit a KIE, assuming HAT is involved in the rate-limiting step of the reaction. The product analysis of the competition assay exhibited a KIE ~2.62 ± 0.21, calculated at the 50 % conversion of the substrate to product (Figure 5C). Recently, a similar observation was reported with a skatole-forming decarboxylase enzyme that follows the HAT mechanism; however, in this case, the KIE calculated from the competition assays was less pronounced (~1.2).[49] In a complementary experiment, we performed the Michaels-Menten kinetics of UndB with d_{23}-LA. We found that the K_m of UndB for d_{23}-LA is 62.28 ± 5.72 μM, and the k_{cat} is 16.10 ± 0.52 min^{-1} (Figure 5D). This result translates to KIE of ~1.5 ± 0.1 on k_{cat} and ~3.29 ± 0.43 on the k_{cat}/K_m, which aligns with the KIE data observed from the competition assay. We note that in a previous study with OleT, a large KIE on the decay of the compound I was observed, which demonstrated the HAT mechanism for OleT.[41] Together, our investigation explored the plausible mechanistic plot of UndB and provided the first evidence in favor of the HAT mechanism for UndB.

Discussion

The discovery of UndB as one of the most efficient enzymes for producing fatty acid-derived alkenes has attracted substantial attention. However, the membrane-bound nature of UndB and the challenges associated with investigating integral membrane proteins impeded the exploration of this enzyme. In the literature, there are only three reported integral membrane enzymes: insect CYP4G1[7], plant CER1[6], and UndB, known to produce fatty-acid-derived hydrocarbons. While insect CYP4G1 and plant CER1 convert very long-chain fatty aldehydes to alkanes[6, 7], UndB is the only integral membrane enzyme known to produce medium-chain 1-alkenes from fatty acids. All these integral membrane enzymes have eluded biochemical and mechanistic characterization, majorly because of the difficulties of purifying these enzymes.[6, 7, 50] In this study, we purified the full-length membrane-bound UndB to homogeneity and performed detailed biochemical characterization of the enzyme for the first time. The metal analysis and the activity assays of the purified enzyme established that UndB is a non-heme diiron enzyme. Through mutational analysis, we identified the key active site residues responsible for binding to the diiron center of the enzyme. Our investigation suggests that UndB is a member of the FADH family of enzymes. Among the members of the FADH family, which utilize fatty acid (or fatty acyl esters) as the substrate, UndB is the only enzyme that performs the decarboxylation chemistry to produce 1-undecene.

To establish UndB activity, we used biological and several chemical redox partners and found that Fdx/FNR/NADPH system supported the *in vitro* activity of UndB. Based on these results and the generic role of Fdx and FNR, we demonstrated that electrons are transferred from NADPH to UndB via FNR and Fdx (Figure 6A) to support the UndB catalysis. Through substrate screening, we established that UndB prefers lauric acid as a substrate. Further, we provided evidence for the UndB-catalyzed oxidative cleavage of the C1-C2 bond of the fatty acid, which led to the release of CO_2 as the C1-derived co-product. We also found that UndB cannot employ the peroxide shunt pathway for catalysis in contrast to SCD1, which was recently reported to utilize H_2O_2 to perform the desaturation reaction[51], suggesting a unique oxygen activation mechanism might be operant in UndB.

Among the 1-alkene-producing metalloenzymes discovered so far, UndA shows very poor *in vitro* activity, proposedly due to the cofactor instability.[38] OleT produces hydroxy-fatty acids as side products along with terminal alkenes.[10, 44] Notably, our kinetic studies of UndB with lauric acid demonstrated that UndB-catalyzed reaction is faster than UndA and OleT for producing medium-chain 1-alkenes. Further, we did not observe any side products in the UndB reaction. Side product formation is not only limited to OleT but is also reported for a number of the members of the FADH family. Alkane monooxygenase (AlkB) is one such enzyme that produces desaturated products along with the hydroxylated products.[52, 53] The side reactions are proposed to happen due to the oxygen insertion or a second hydrogen abstraction after the initial HAT, resulting in hydroxylated or desaturated side products, respectively. Previous studies have elegantly showed that substrate binding and active site features could alter the specificity of the reactions leading to side-product formations.[42, 43, 54] The absence of side products in the UndB reaction suggests that UndB catalysis is tightly regulated.

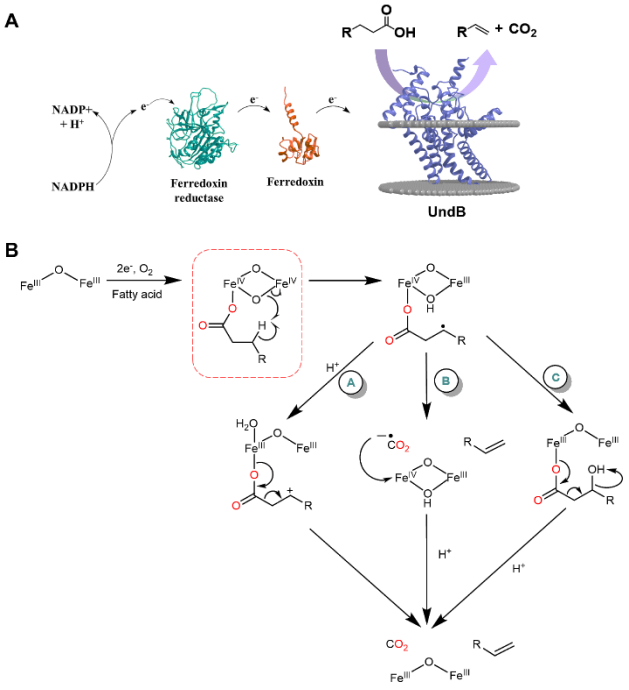

Figure 6. Proposed pathway and mechanism of UndB-catalyzed fatty acid decarboxylation. (A) Electrons transfer from NADPH to UndB via ferredoxin reductase and ferredoxin. The electron transfer supports the catalysis of UndB. (B) Proposed mechanism of UndB-catalyzed decarboxylation of fatty acids. The HAT step is highlighted with a red box.

Members of the FADH family are proposed to initiate the reaction via a HAT mechanism by an iron-oxo intermediate.[53, 55, 56] This proposition is mainly based on the similarities with soluble desaturases and a few mechanistic studies on this family's other members, such as AlkB and XylM (xylene monooxygenase). [53, 56] Therefore, a similar mechanism might be involved in the decarboxylation reaction of UndB as proposed for desaturation and hydroxylation catalyzed by other enzymes of this family.[56] During the mechanistic studies of UndB, we observed a significant KIE in the assays carried out with the deuterated substrate. Based on our findings and the similarity of UndB with other diiron enzymes, we postulate that UndB initiates the reaction by HAT from the β-carbon of the substrate, which is ultimately lost from the fatty acid to generate 1-alkene. The step following HAT in UndB catalysis would differ from other enzymes such as SCD1, AlkB, or XylM to allow decarboxylation to operate rather than desaturation or hydroxylation. The subsequent step to HAT in UndB might follow one of the possible routes proposed for OleT or UndA[38, 42]: (A) electron transfer to the diiron (III/IV) complex followed by decarboxylation, (B) cleavage of the radicaloid C1–C2 carbons followed by an electron transfer from $CO_2^{\bullet-}$ radical to the diiron (III/IV) complex or, (C) oxygen rebound followed by Grob-type multibond fragmentation (Figure 6B), leading to the formation of the terminal alkene, the release of CO_2, and regeneration of the active site for the subsequent turnover.

Conclusion

1-Alkenes are a significant class of chemicals that find utilities in various industries. Importantly, medium-chain 1-alkenes can also serve as the next-generation hydrocarbon-based drop-in biofuels. Therefore, studying enzymes capable of producing medium-chain 1-alkenes from cheap feedstocks such as fatty acids is of great interest globally. In this study, we presented the first comprehensive analysis of the purification, biochemical characterization, and mechanistic aspects of UndB, the only known membrane-bound 1-alkene-producing enzyme that remained enigmatic for nearly a decade. Our investigation revealed that UndB is a non-heme diiron enzyme that employs conserved histidine residues at the active site and catalyzes the conversion of free fatty acids to 1-alkenes. We demonstrated that UndB is a redox-dependent enzyme, and the activity of UndB is supported by the ferredoxin/ferredoxin reductase/NADPH system. Our substrate screening study identified lauric acid as the preferred substrate for UndB. We also uncovered that UndB carries out the oxidative cleavage of the C1-C2 bond of the fatty acid, releasing CO_2 as the C1-derived co-product. Subsequently, we delineated a plausible mechanistic plot for the UndB-catalyzed reaction. The observation of a significant KIE with deuterated substrate suggested that UndB initiates the reaction by HAT from the β-carbon of the substrate, ultimately resulting in the loss of CO_2 and production of 1-alkene.

Overall, our study provides the first in-depth understanding of the biochemical and catalytic properties of UndB, the only known membrane-bound fatty acid decarboxylase. Our results provide a firm foundation for further structural and mechanistic characterization of UndB, and also open up the possibility of utilizing this enzyme for biotechnological applications, particularly in the biosynthesis of 1-alkenes, which have numerous industrial applications. Additionally, our approach to investigating the UndB enzyme could be extended to elucidate the functions of other enigmatic membrane-bound metalloenzymes.

ASSOCIATED CONTENT

Supporting Information.
Full description of materials, detailed methods for plasmid construction, protein expression and purification, characterization, biochemical assays, GC-MS analysis, and chromatograms.
Figures S1−S26, and Tables S1−S4 (PDF)
"This material is available free of charge via the Internet at http://pubs.acs.org

AUTHOR INFORMATION

Corresponding Author

*Debasis Das− Department of Inorganic and Physical Chemistry, Indian Institute of Science, Bangalore-560012, India. orcid.org/0000-0001-8967-3348; Email: debasisdas@iisc.ac.in; Phone No.: +918022933002

Present Addresses

[1]Department of Inorganic and Physical Chemistry, Indian Institute of Science, Bangalore-560012, India.

Author Contributions

D.D. and T.I. conceived the project and designed the experiments. T.I. and S.M. carried out molecular biology experiments, enzyme expression and purification, enzyme characterization, enzyme assays, and bioinformatics studies and presented the data. K.R., T.I., and S.M. performed the expression and purification of the redox partner proteins. T.I., S. M., and J.S.S. contributed to new materials and carried out substrate-dependent studies. D.D., T.I., and S.M. analyzed the data and wrote the manuscript. All authors discussed the results, reviewed, and edited the manuscript.

Funding Sources

This work was financially supported by the Science and Engineering Research Board (CRG/2019/000943), India, and the Indian Institute of Science (IISc), Bangalore, India, (SR/MHRD-18-0021).

Notes

The authors declare no competing financial interest.

ACKNOWLEDGMENT

The authors thank Prof. Shengying Li (Shandong University, China) for kindly providing the expression plasmid harboring Fdx and FNR. The authors also thank Prof. Barbara Imperiali (MIT, USA) for the kind gifts of plasmids containing genes encoding TEV protease. The authors thank Prof. Aravind Penmatsa (IISc, India) for the kind gift of the plasmids. The authors thank Prof. Ramananda Chakrabarti, Centre for Earth Sciences (IISc, India) for the ICP-MS facility and the Spectroscopy Analytical Test Facility (IISc, India) for the ICP-OES facility.

REFERENCES

1. Peralta-Yahya, P. P.; Zhang, F.; del Cardayre, S. B.; Keasling, J. D., Microbial engineering for the production of advanced biofuels. *Nature* **2012,** *488* (7411), 320-328.
2. Liao, J. C.; Mi, L.; Pontrelli, S.; Luo, S., Fuelling the future: microbial engineering for the production of sustainable biofuels. *Nat. Rev. Microbiol.* **2016,** *14* (5), 288-304.
3. Zhou, Y. J.; Kerkhoven, E. J.; Nielsen, J., Barriers and opportunities in bio-based production of hydrocarbons. *Nat. Energy* **2018,** *3* (11), 925-935.
4. Liu, K.; Li, S., Biosynthesis of fatty acid-derived hydrocarbons: perspectives on enzymology and enzyme engineering. *Curr. Opin. Biotechnol.* **2020,** *62*, 7-14.
5. Iqbal, T.; Chakraborty, S.; Murugan, S.; Das, D., Metalloenzymes for fatty acid-derived hydrocarbon biosynthesis: nature's cryptic catalysts. *Chem. Asian J.* **2022,** *17*, e202200105.
6. Bernard, A.; Domergue, F.; Pascal, S.; Jetter, R.; Renne, C.; Faure, J. D.; Haslam, R. P.; Napier, J. A.; Lessire, R.; Joubes, J., Reconstitution of plant alkane biosynthesis in yeast demonstrates that Arabidopsis eceriferum1 and eceriferum3 are core components of a very-long-chain alkane synthesis complex. *Plant Cell* **2012,** *24* (7), 3106-3118.
7. Qiu, Y.; Tittiger, C.; Wicker-Thomas, C.; Le Goff, G.; Young, S.; Wajnberg, E.; Fricaux, T.; Taquet, N.; Blomquist, G. J.; Feyereisen, R., An insect-specific P450 oxidative decarbonylase for cuticular hydrocarbon biosynthesis. *Proc. Natl. Acad. Sci. U.S.A.* **2012,** *109* (37), 14858-14863.
8. Schirmer, A.; Rude, M. A.; Li, X.; Popova, E.; del Cardayre, S. B., Microbial biosynthesis of alkanes. *Science* **2010,** *329* (5991), 559-562.
9. Sorigue, D.; Legeret, B.; Cuine, S.; Blangy, S.; Moulin, S.; Billon, E.; Richaud, P.; Brugiere, S.; Coute, Y.; Nurizzo, D.; Muller, P.; Brettel, K.; Pignol, D.; Arnoux, P.; Li-Beisson, Y.; Peltier, G.; Beisson, F., An algal photoenzyme converts fatty acids to hydrocarbons. *Science* **2017,** *357* (6354), 903-907.
10. Rude, M. A.; Baron, T. S.; Brubaker, S.; Alibhai, M.; Del Cardayre, S. B.; Schirmer, A., Terminal olefin (1-alkene) biosynthesis by a novel p450 fatty acid decarboxylase from Jeotgalicoccus species. *Appl. Environ. Microbiol.* **2011,** *77* (5), 1718-1727.
11. Rui, Z.; Li, X.; Zhu, X.; Liu, J.; Domigan, B.; Barr, I.; Cate, J. H.; Zhang, W., Microbial biosynthesis of medium-chain 1-alkenes by a nonheme iron oxidase. *Proc. Natl. Acad. Sci. U.S.A.* **2014,** *111* (51), 18237-18242.
12. Rui, Z.; Harris, N. C.; Zhu, X. J.; Huang, W.; Zhang, W. J., Discovery of a family of desaturase-like enzymes for 1-alkene biosynthesis. *ACS Catal.* **2015,** *5* (12), 7091-7094.
13. Ray, S.; Rao, P. V. C.; Choudary, N. V., Poly-alpha-olefin-based synthetic lubricants: a short review on various synthetic routes. *Lubr. Sci.* **2012,** *24* (1), 23-44.
14. Lappin, G., *Alpha Olefins Applications Handbook*. CRC press: Boca Raton, 2014.
15. Blackwell, J.; Bullen, J.; Shubkin, R., Current and future polyalphaolefins. *J. Synth. Lubr.* **1990,** *7* (1), 25-45.
16. Benda, R.; Bullen, J.; Plomer, A., Synthetics basics: polyalphaolefins—base fluids for high-performance lubricants. *J. Synth. Lubr.* **1996,** *13* (1), 41-57.
17. Manley, O. M.; Fan, R.; Guo, Y.; Makris, T. M., Oxidative decarboxylase UndA utilizes a dinuclear iron cofactor. *J. Am. Chem. Soc.* **2019,** *141* (22), 8684-8688.
18. Lin, Y. T.; Stańczak, A.; Manchev, Y.; Straganz, G. D.; de Visser, S. P., Can a mononuclear iron (III)-superoxo active site catalyze the decarboxylation of dodecanoic acid in UndA to produce biofuels? *Chem. Eur. J.* **2020,** *26* (10), 2233-2242.
19. Zhou, Y. J. J.; Hu, Y. T.; Zhu, Z. W.; Siewers, V.; Nielsen, J., Engineering 1-alkene biosynthesis and secretion by dynamic regulation in yeast. *ACS Synth. Biol.* **2018,** *7* (2), 584-590.
20. Wang, J.; Yu, H.; Zhu, K., Employing metabolic engineered lipolytic microbial platform for 1-alkene one-step conversion. *Bioresour. Technol.* **2018,** *263*, 172-179.
21. Wu, S. K.; Zhou, Y.; Gerngross, D.; Jeschek, M.; Ward, T. R., Chemo-enzymatic cascades to produce cycloalkenes from bio-based resources. *Nat. Commun.* **2019,** *10*.
22. Intasian, P.; Prakinee, K.; Phintha, A.; Trisrivirat, D.; Weeranoppanant, N.; Wongnate, T.; Chaiyen, P., Enzymes, in vivo biocatalysis, and metabolic engineering for enabling a circular economy and sustainability. *Chem. Rev.* **2021,** *121* (17), 10367-10451.
23. Shanklin, J.; Whittle, E.; Fox, B. G., Eight histidine residues are catalytically essential in a membrane-associated iron enzyme, stearoyl-CoA desaturase, and are conserved in alkane hydroxylase and xylene monooxygenase. *Biochemistry* **1994,** *33* (43), 12787-12794.
24. Arthington, B. A.; Bennett, L. G.; Skatrud, P. L.; Guynn, C. J.; Barbuch, R. J.; Ulbright, C. E.; Bard, M., Cloning, disruption and sequence of the gene encoding yeast c-5 sterol desaturase. *Gene* **1991,** *102* (1), 39-44.
25. Bai, Y. H.; McCoy, J. G.; Levin, E. J.; Sobrado, P.; Rajashankar, K. R.; Fox, B. G.; Zhou, M., X-ray structure of a mammalian stearoyl-CoA desaturase. *Nature* **2015,** *524* (7564), 252-256.
26. Shen, J.; Wu, G.; Tsai, A. L.; Zhou, M., Structure and mechanism of a unique diiron center in mammalian stearoyl-coa desaturase. *J. Mol. Biol.* **2020,** *432* (18), 5152-5161.
27. Shanklin, J.; Guy, J. E.; Mishra, G.; Lindqvist, Y., Desaturases: emerging models for understanding functional diversification of diiron-containing enzymes. *J. Biol. Chem.* **2009,** *284* (28), 18559-18563.
28. Jasniewski, A. J.; Que, L., Dioxygen activation by nonheme diiron enzymes: diverse dioxygen adducts, high-valent intermediates, and related model complexes. *Chem. Rev.* **2018,** *118* (5), 2554-2592.
29. de Rond, T.; Stow, P.; Eigl, I.; Johnson, R. E.; Chan, L. J. G.; Goyal, G.; Baidoo, E. E. K.; Hillson, N. J.; Petzold, C. J.; Sarpong, R.; Keasling, J. D., Oxidative cyclization of prodigiosin by an alkylglycerol monooxygenase-like enzyme. *Nat. Chem. Biol.* **2017,** *13* (11), 1155-1157.
30. Das, D.; Eser, B. E.; Han, J.; Sciore, A.; Marsh, E. N., Oxygen-independent decarbonylation of aldehydes by cyanobacterial aldehyde decarbonylase: a new reaction of diiron enzymes. *Angew. Chem. Int. Ed.* **2011,** *50* (31), 7148-52.
31. Stookey, L. L., Ferrozine - a new spectrophotometric reagent for iron. *Anal. Chem.* **1970,** *42* (7), 779-781.
32. Jumper, J.; Evans, R.; Pritzel, A.; Green, T.; Figurnov, M.; Ronneberger, O.; Tunyasuvunakool, K.; Bates, R.; Zidek, A.; Potapenko, A.; Bridgland, A.; Meyer, C.; Kohl, S. A. A.; Ballard, A. J.; Cowie, A.; Romera-Paredes, B.; Nikolov, S.; Jain, R.; Adler, J.; Back, T.; Petersen, S.; Reiman, D.; Clancy, E.; Zielinski, M.; Steinegger, M.; Pacholska, M.; Berghammer, T.; Bodenstein, S.; Silver, D.; Vinyals, O.; Senior, A. W.; Kavukcuoglu, K.; Kohli, P.; Hassabis, D., Highly accurate protein structure prediction with AlphaFold. *Nature* **2021,** *596* (7873), 583-589.
33. Mirdita, M.; Schutze, K.; Moriwaki, Y.; Heo, L.; Ovchinnikov, S.; Steinegger, M., ColabFold: making protein folding accessible to all. *Nat. Methods* **2022,** *19* (6), 679-682.
34. Lomize, M. A.; Pogozheva, I. D.; Joo, H.; Mosberg, H. I.; Lomize, A. L., OPM database and PPM web server: resources for positioning of proteins in membranes. *Nucleic Acids Res.* **2012,** *40* (D1), D370-D376.
35. Zhu, G.; Koszelak-Rosenblum, M.; Connelly, S. M.; Dumont, M. E.; Malkowski, M. G., The crystal structure of an integral membrane fatty acid alpha-hydroxylase. *J. Biol. Chem.* **2015,** *290* (50), 29820-33.
36. Liu, Y.; Wang, C.; Yan, J.; Zhang, W.; Guan, W.; Lu, X.; Li, S., Hydrogen peroxide-independent production of alpha-alkenes by OleTJE P450 fatty acid decarboxylase. *Biotechnol. Biofuels* **2014,** *7* (1), 28.
37. Andre, C.; Kim, S. W.; Yu, X. H.; Shanklin, J., Fusing catalase to an alkane-producing enzyme maintains enzymatic activity by converting the inhibitory byproduct H2O2 to the cosubstrate O2. *Proc. Natl. Acad. Sci. U.S.A.* **2013,** *110* (8), 3191-3196.

38. Zhang, B.; Rajakovich, L. J.; Van Cura, D.; Blaesi, E. J.; Mitchell, A. J.; Tysoe, C. R.; Zhu, X.; Streit, B. R.; Rui, Z.; Zhang, W.; Boal, A. K.; Krebs, C.; Bollinger, J. M., Jr., Substrate-triggered formation of a peroxo-Fe2(III/III) intermediate during fatty acid decarboxylation by UndA. *J. Am. Chem. Soc.* **2019,** *141* (37), 14510-14514.
39. Pandelia, M. E.; Li, N.; Norgaard, H.; Warui, D. M.; Rajakovich, L. J.; Chang, W. C.; Booker, S. J.; Krebs, C.; Bollinger, J. M., Jr., Substrate-triggered addition of dioxygen to the diferrous cofactor of aldehyde-deformylating oxygenase to form a diferric-peroxide intermediate. *J. Am. Chem. Soc.* **2013,** *135* (42), 15801-15812.
40. Warui, D. M.; Li, N.; Nørgaard, H.; Krebs, C.; Bollinger, J. M.; Booker, S. J., Detection of formate, rather than carbon monoxide, as the stoichiometric coproduct in conversion of fatty aldehydes to alkanes by a cyanobacterial aldehyde decarbonylase. *J. Am. Chem. Soc.* **2011,** *133* (10), 3316-3319.
41. Grant, J. L.; Hsieh, C. H.; Makris, T. M., Decarboxylation of fatty acids to terminal alkenes by cytochrome p450 compound I. *J. Am. Chem. Soc.* **2015,** *137* (15), 4940-4943.
42. Grant, J. L.; Mitchell, M. E.; Makris, T. M., Catalytic strategy for carbon-carbon bond scission by the cytochrome P450 OleT. *Proc. Natl. Acad. Sci. U.S.A.* **2016,** *113* (36), 10049-10054.
43. Wise, C. E.; Hsieh, C. H.; Poplin, N. L.; Makris, T. M., Dioxygen activation by the biofuel-generating cytochrome P450 OleT. *ACS Catal.* **2018,** *8* (10), 9342-9352.
44. Hsieh, C. H.; Huang, X. Y.; Amaya, J. A.; Rutland, C. D.; Keys, C. L.; Groves, J. T.; Austin, R. N.; Makris, T. M., The enigmatic p450 decarboxylase OleT is capable of, but evolved to frustrate, oxygen rebound chemistry. *Biochemistry* **2017,** *56* (26), 3347-3357.
45. Rajakovich, L. J.; Norgaard, H.; Warui, D. M.; Chang, W. C.; Li, N.; Booker, S. J.; Krebs, C.; Bollinger, J. M., Jr.; Pandelia, M. E., Rapid reduction of the diferric-peroxyhemiacetal intermediate in aldehyde-deformylating oxygenase by a cyanobacterial ferredoxin: evidence for a free-radical mechanism. *J. Am. Chem. Soc.* **2015,** *137* (36), 11695-11709.
46. Paul, B.; Das, D.; Ellington, B.; Marsh, E. N. G., Probing the mechanism of cyanobacterial aldehyde decarbonylase using a cyclopropyl aldehyde. *J. Am. Chem. Soc.* **2013,** *135* (14), 5234-5237.
47. Peters, R.; Hellenbrand, J.; Mengerink, Y.; Van der Wal, S., On-line determination of carboxylic acids, aldehydes and ketones by high-performance liquid chromatography-diode array detection-atmospheric pressure chemical ionisation mass spectrometry after derivatization with 2-nitrophenylhydrazine. *J. Chromatogr. A* **2004,** *1031* (1-2), 35-50.
48. Yadav, S.; Shaik, S.; Siddiqui, S. A.; Kalita, S.; Dubey, K. D., Local electric fields dictate function: the different product selectivities observed for fatty acid oxidation by two deceptively very similar P450-peroxygenases OleT and BSβ. *J. Chem. Inf. Model.* **2022,** *62* (4), 1025-1035.
49. Fu, B.; Nazemi, A.; Levin, B. J.; Yang, Z.; Kulik, H. J.; Balskus, E. P., Mechanistic studies of a skatole-forming glycyl radical enzyme suggest reaction initiation via hydrogen atom transfer. *J. Am. Chem. Soc.* **2022,** *144* (25), 11110-11119.
50. Schneider-Belhaddad, F.; Kolattukudy, P., Solubilization, partial purification, and characterization of a fatty aldehyde decarbonylase from a higher plant, Pisum sativum. *Arch. Biochem. Biophys.* **2000,** *377* (2), 341-349.
51. Shen, J.; Wu, G.; Tsai, A.-L.; Zhou, M., Mammalian stearoyl-Coa desaturase forms a stable ternary complex with cytochrome b5 and cytochrome b5 reductase. *Biophys. J.* **2020,** *118* (3), 524a.
52. Cooper, H. L.; Mishra, G.; Huang, X.; Pender-Cudlip, M.; Austin, R. N.; Shanklin, J.; Groves, J. T., Parallel and competitive pathways for substrate desaturation, hydroxylation, and radical rearrangement by the non-heme diiron hydroxylase AlkB. *J. Am. Chem. Soc.* **2012,** *134* (50), 20365-20375.
53. Austin, R. N.; Chang, H.-K.; Zylstra, G. J.; Groves, J. T., The non-heme diiron alkane monooxygenase of Pseudomonas leovorans (AlkB) hydroxylates via a substrate radical intermediate. *J. Am. Chem. Soc.* **2000,** *122* (47), 11747-11748.
54. Fang, B.; Xu, H.; Liu, Y.; Qi, F.; Zhang, W.; Chen, H.; Wang, C.; Wang, Y.; Yang, W.; Li, S., Mutagenesis and redox partners analysis of the P450 fatty acid decarboxylase OleTJE. *Sci. Rep.* **2017,** *7* (1), 1-7.
55. Austin, R. N.; Buzzi, K.; Kim, E.; Zylstra, G. J.; Groves, J. T., Xylene monooxygenase, a membrane-spanning non-heme diiron enzyme that hydroxylates hydrocarbons via a substrate radical intermediate. *J. Biol. Inorg. Chem.* **2003,** *8* (7), 733-740.
56. Wise, C. E.; Grant, J. L.; Amaya, J. A.; Ratigan, S. C.; Hsieh, C. H.; Manley, O. M.; Makris, T. M., Divergent mechanisms of iron-containing enzymes for hydrocarbon biosynthesis. *J. Biol. Inorg. Chem.* **2017,** *22* (2), 221-235.